



**HAL**  
open science

# Bacteria-derived peptidoglycan triggers a non-canonical NF- $\kappa$ B dependent response in *Drosophila* gustatory neurons

Ambra Masuzzo, Gérard Manière, Yael Grosjean, Léopold Kurz, Julien Royet

► **To cite this version:**

Ambra Masuzzo, Gérard Manière, Yael Grosjean, Léopold Kurz, Julien Royet. Bacteria-derived peptidoglycan triggers a non-canonical NF- $\kappa$ B dependent response in *Drosophila* gustatory neurons. *Journal of Neuroscience*, 2022, 42 (41), pp.7809-7823. 10.1523/JNEUROSCI.2437-21.2022 . hal-03813389

**HAL Id: hal-03813389**

**<https://hal.inrae.fr/hal-03813389>**

Submitted on 24 Nov 2022

**HAL** is a multi-disciplinary open access archive for the deposit and dissemination of scientific research documents, whether they are published or not. The documents may come from teaching and research institutions in France or abroad, or from public or private research centers.

L'archive ouverte pluridisciplinaire **HAL**, est destinée au dépôt et à la diffusion de documents scientifiques de niveau recherche, publiés ou non, émanant des établissements d'enseignement et de recherche français ou étrangers, des laboratoires publics ou privés.

801  
802  
803  
804  
805  
806  
807  
808  
809  
810  
811  
812  
813  
814  
815  
816  
817  
818  
819  
820

**Bacteria-derived peptidoglycan triggers a non-canonical NF- $\kappa$ B dependent response in *Drosophila* gustatory neurons**

Ambra Masuzzo<sup>1 §</sup>, Gérard Manière<sup>2 §</sup>, Yaël Grosjean<sup>2 \*</sup>, Léopold Kurz<sup>1 \*</sup>, Julien Royet<sup>1 \*</sup>

1 : Aix-Marseille Université, CNRS, IBDM, Marseille, France

2 : Centre des Sciences du Goût et de l'Alimentation, L'Institut agro Dijon, CNRS, INRAE,  
Université Bourgogne Franche-Comté, F-21000 Dijon, France

<sup>§</sup> co-first author, <sup>\*</sup> co-corresponding authors

Abbreviated title: Bacteria-derived peptidoglycan sensing by gustatory neurons

821 **Abstract**

822

823 Probing the external world is essential for eukaryotes to distinguish beneficial from pathogenic  
824 microorganisms. If it is clear that the main part of this task falls to the immune cells, recent  
825 work shows that neurons can also detect microbes, although the molecules and mechanisms  
826 involved are less characterized. In *Drosophila*, detection of bacteria-derived peptidoglycan by  
827 pattern recognition receptors of the PGRP family expressed in immune cells, triggers NF-  
828  $\kappa$ B/IMD dependent signaling. We show here that one PGRP protein, called PGRP-LB, is ex-  
829 pressed in some proboscis's bitter gustatory neurons. *In vivo* calcium imaging in female flies  
830 reveals that the PGRP/IMD pathway is cell-autonomously required in these neurons to trans-  
831 duce the peptidoglycan signal. We finally show that NF- $\kappa$ B/IMD pathway activation in bitter-  
832 sensing gustatory neurons influences fly behavior. This demonstrates that a major immune re-  
833 sponse elicitor and signaling module are required in the peripheral nervous system to sense the  
834 presence of bacteria in the environment.

835

836

837 **Significance**

838

839 In addition to the classical immune response, eukaryotes rely on neuronally-controlled mecha-  
840 nisms to detect microbes and engage in adapted behaviors. However, the mechanisms of mi-  
841 crobe detection by the nervous system are poorly understood. Using genetic analysis and cal-  
842 cium imaging, we demonstrate here that bacteria-derived peptidoglycan can activate bitter gus-  
843 tatory neurons. We further show that this response is mediated by the PGRP-LC membrane  
844 receptor and downstream components of a non-canonical NF- $\kappa$ B signaling cascade. Activation  
845 of this signaling cascade triggers behavior changes. These data demonstrate that bitter-sensing  
846 neurons and immune cells share a common detection and signaling module to either trigger the  
847 production of antibacterial effectors or to modulate the behavior of flies that are in contact with  
848 bacteria. Since PGN detection doesn't mobilize the known gustatory receptors, it also demon-  
849 strates that taste perception is much more complex than anticipated

850

851

852 **Introduction**

853

854 Since microorganisms can reduce the fitness of their hosts, natural selection has favored defense  
855 mechanisms that protect them against disease-causing agents. The molecular mechanisms that  
856 are activated during the humoral and cellular responses, the main armed branches of the host  
857 against invading microbes, are known in great detail. By avoiding pathogenic microorganisms  
858 or modifying its behavior when infected, host can prevent the activation of the costly immune  
859 response, maximizes its efficiency and reduce the consequences of the infection on themselves  
860 or their progeny. Phenotypes related to such behaviors are well known in mammals. They range  
861 from disgust to social isolation including sleepiness <sup>1</sup>. These responses to the microbial envi-  
862 ronment are accepted as symptoms, but are not well defined molecularly. Observations in in-  
863 vertebrates phenocopying the mammalian sickness behaviors have also been made <sup>2</sup> and may  
864 often be interpreted in an anthropomorphic way while there is no molecular deciphering or no  
865 ecological context. For instance, social insects, such as termites can ascertain the virulence of  
866 the *Metarhizium* and *Beauveria* fungi and avoid the most virulent strains<sup>3</sup>, while *Apis mellifera*  
867 workers are able to detect larvae infected with the fungus *Ascosphaera apis* and remove them  
868 from the nest<sup>4</sup>. On the other hand, since some microorganisms are beneficial for their host,  
869 animals can also be attracted by them. Up to date, the molecular and neuronal basis of these  
870 behavioral responses to microbes are much less characterized than the “canonical” immune  
871 responses. Genetically tractable models such as *Caenorhabditis elegans* or *Drosophila mela-*  
872 *nogaster* are very well suited to elucidate them <sup>5, 6, 7, 8</sup>.

873         Devoid of adaptative immunity like all invertebrates, *Drosophila* has emerged as a well-  
874 adapted model to unravel the signaling modules that control the innate immune responses  
875 against bacteria <sup>9, 10, 11, 12</sup>. Essential to them are two NF-κB signaling pathways called Toll and  
876 IMMune Deficiency (IMD) whose activation triggers the production of immune effectors, such  
877 as AntiMicrobial Peptides (AMPs), in immune-competent cells <sup>9, 13, 14, 15</sup>. This activation de-  
878 pends on the previous detection of bacteria-derived PeptidoGlycaN (PGN) by host Pattern  
879 Recognition Receptors (PRRs) belonging to the PeptidoGlycan Recognition Protein (PGRP)  
880 family <sup>16, 17</sup>. Recent work has shown that signaling components of the NF-κB/IMD pathway,  
881 including the NF-κB transcription factor Relish, and the upstream PGRP sensors are function-  
882 ally required outside the immune system and more specifically in some neurons of the Central  
883 Nervous System (CNS) <sup>18, 19</sup>. Direct recognition of circulating bacteria-derived PGN by few  
884 brain octopaminergic neurons leads to their inhibition and, in turn, to an egg-laying reduction

885 in PGN-exposed females <sup>20 19</sup>. Hence, by detecting a ubiquitous bacteria cell wall component  
886 via dedicated PRRs, few brain neurons adapt the female physiology to its infectious status.

887 The Peripheral Nervous System (PNS) of *Drosophila* and more specifically its gustatory  
888 and olfactory systems are also involved in microbe-induced behaviors. By activating a subclass  
889 of olfactory neurons that express the olfactory receptor Or56a, the microbial odorant geosmin  
890 induces pathogen avoidance by inhibiting oviposition, chemotaxis, and feeding <sup>21</sup>. In contrast,  
891 bacterial volatiles commonly produced during decomposition of plant material such as ammo-  
892 nia and certain amines, are highly attractive to flies <sup>22</sup>. Furthermore, Or30a-dependent detection  
893 of bacteria-derived short-chain fatty acid induces attraction in larvae<sup>23</sup>. Previous works demon-  
894 strated that bacterial cell wall components like LipoPolySaccharide (LPS) and PGN are de-  
895 tected by *Drosophila*'s gustatory sensory system <sup>24</sup>. Detection of LPS by the esophageal bitter  
896 Gustatory Receptor Neurons (GRNs) expressing the chemosensory cation channel TrpA1  
897 (Transient receptor potential cation channel subfamily A member 1) triggers feeding and ovi-  
898 position avoidance <sup>25</sup>. PGN detection, instead, triggers grooming behavior upon stimulation of  
899 wing margins and legs but the nature of gustatory sensory neurons and receptors involved in  
900 this behavior remain elusive <sup>24</sup>.

901 Previous work has shown that recognition of bacteria-derived PGN by fly PGRPs me-  
902 diates many of these procaryotes-eucaryotes interactions. Di-Amino Pimelic PGN (DAP-type  
903 PGN) found in the cell wall of most Gram-negative bacteria is detected either at the membrane  
904 of immune competent cells by PGRP-LC, or in the cytosol by the soluble PGRP-LE receptor  
905 <sup>26, 27, 28</sup>. In both cases, this recognition step is sufficient to activate the evolutionary conserved  
906 NF- $\kappa$ B downstream signaling cascade that, in turn, will induce the production of antibacterial  
907 molecules. Probably because its prolonged activation is detrimental for the host, NF- $\kappa$ B path-  
908 way activation levels are finely modulated by several negative regulators <sup>29</sup>. Among them are  
909 enzymes, called amidases, that by binding and cleaving the PGN into inactive products buffer  
910 IMD pathway activation. PGRP-LB is such an enzyme that is present either extracellularly via  
911 its PGRP-LB<sup>RC</sup> isoform or inside the cell via the PGRP-LB<sup>RA</sup> and <sup>RD</sup> isoforms<sup>30, 31, 32, 33</sup>. We  
912 present here data demonstrating that the PGRP-LB enzyme and other IMD pathway compo-  
913 nents are expressed in some gustatory neurons suggesting that these cells might sense and react  
914 to external PGN. Using genetic analysis and calcium imaging, we demonstrate that some mem-  
915 bers of the IMD pathway are functionally required in bitter-sensing gustatory neurons to sense  
916 and transduce the presence of PGN without the mobilization of the classical gustatory receptors  
917 expressed in these cells. These results demonstrate that the taste system can be used by the fly  
918 to detect the presence of PGN in the environment and that the PGRP/IMD module is not only

919 required in immune cells to trigger the production of antibacterial effectors but also in sensory  
920 neurons to modulate fly behavior upon bacteria sensing. Thus, the PGN that is used as an alarm  
921 signal when detected within the body cavity is as well a qualitative readout about the fly envi-  
922 ronment.

923

924

## 925 **Results**

### 926 **A peptidoglycan binding protein is expressed in some bitter gustatory neurons**

927 Our previous work has shown that some PGN sensing molecules (PGRPs) are active outside  
928 immune cells and specifically in neurons of the CNS. Indeed, the direct detection of bacteria-  
929 derived PGN by the cytosolic protein PGRP-LE in a subset of brain octopaminergic neurons  
930 modulates oviposition of infected females in an NF- $\kappa$ B-dependent manner<sup>18, 20</sup>. To identify  
931 neurons which potentially expressed PGRPs and thus respond to PGN, we previously made use  
932 of a reporter line, pLB1<sup>Gal4</sup>, that partially recapitulates the endogenous expression of one PGRP-  
933 LB protein isoform (i.e., PGRP-LB<sup>RD</sup>)<sup>20</sup> (Extended Data Fig.1-1a). We now noticed that, in  
934 addition to being expressed in some neurons of the brain, this line also labeled axonal projec-  
935 tions that originated from neurons of the PNS. In pLB1<sup>Gal4</sup>/UAS-mCD8-GFP flies, a GFP signal  
936 was observed in the Sub-Esophageal Zone (SEZ) of the central brain where GRNs send their  
937 axonal projections (Fig. 1a, b)<sup>34, 35</sup>. Accordingly, some sparse cell bodies present in the labella  
938 at the position of taste sensory neurons were detected (here called pLB1+ neurons; Fig. 1c,  
939 Extended data Fig. 1-1b and Table 1). In contrast, no signal was detected using the two other  
940 PGRP-LB isoform reporter constructs pLB2<sup>Gal4</sup> and pLB3<sup>Gal4</sup> (Extended Data Fig.1-1a, b)<sup>18</sup>.  
941 The axonal network within the SEZ of pLB1<sup>Gal4</sup>/UAS-mCD8-GFP flies is reminiscent of taste  
942 neurons associated with detection of molecules triggering aversion and classified as bitter. Dou-  
943 ble staining between pLB1<sup>Gal4</sup>/UAS-mCD8-GFP and Gr66a-RFP, which is specifically ex-  
944 pressed in bitter gustatory neurons, revealed that all pLB1+ neurons are bitter (Gr66a+), alt-  
945 hough they only represent a sub-population of them (Fig. 1d, e and Table 2). Indeed, while there  
946 are around 25 Gr66a+ neurons per each labellum, we identified an average of  $5 \pm 2$  pLB1+  
947 neurons<sup>36, 37, 38</sup> (Table 1 and Table 2). We confirmed this result by using genetic intersectional  
948 strategy between pLB1<sup>Gal4</sup> and Gr66a<sup>LexA</sup> (Extended Data Fig. 1-2a) and by using another driver  
949 that broadly targets bitter-sensing gustatory neurons (i.e., Gr32a<sup>LexA</sup>) (Extended Data Fig. 1-  
950 2c). Consistently, by using the same strategy and a driver that labels sweet GRNs (Gr5a<sup>LexA</sup>),  
951 we did not detect any neurons that are simultaneously pLB1+ and Gr5a+ (Extended Data Fig.  
952 1-2d). In addition, the expression of the Gal4 inhibitor Gal80 in Gr66a+ neurons

953 (Gr66a<sup>LexA/LexAop<sup>Gal80</sup></sup>) suppressed the expression of GFP in pLB1+ neurons (pLB1<sup>Gal4</sup>/UAS-  
954 mCD8-GFP). No signal was detected in pLB1<sup>Gal4</sup>/UAS-mCD8-GFP flies expressing the Gal80  
955 repressor, (Extended Data Fig. 1-2b). Lastly, imaging using a pan-isoform reporter line in which  
956 the endogenous PGRP-LB has been GFP-tagged at the locus (PGRP-LB::GFP) demonstrated  
957 that the endogenous PGRP-LB protein is also produced in Gr66a+ neurons (Extended Data Fig.  
958 1-2e). Taken together, these data demonstrate that all the pLB1+ neurons in the proboscis are  
959 bitter-sensing neurons.

960

### 961 **Bitter GRNs respond to bacteria and to DAP-type PGN**

962 Since we observed in bitter-sensing gustatory neurons the expression of an enzyme dedicated  
963 to the buffering of the NF- $\kappa$ B/IMD response and that the PGN is a proxy to delineate whether  
964 bacteria are present or not, we first tested whether pLB1+ gustatory neurons could be activated  
965 by bacterial PGN by performing *in vivo* calcium imaging.

966 Two types of PGN, which differs for a single amino acid in the stem peptide, are found in  
967 bacteria. Whereas the Lysine (Lys)-type PGN is found in Gram-positive bacteria cell wall, the  
968 DAP-type PGN forms that of Gram-negative bacteria. While Lys-type PGN preferentially trig-  
969 gers the *Drosophila* NF- $\kappa$ B/Toll pathway, DAP-type PGN mainly leads to the activation of the  
970 NF- $\kappa$ B/IMD pathway<sup>26</sup>. Exposing the labella of pLB1<sup>Gal4</sup>/UAS-GCaMP6s flies to DAP-type  
971 PGN triggered an increase of the intracellular calcium levels in the SEZ located axonal projec-  
972 tions of labellar pLB1+ neurons, indicating that this subset of gustatory neurons senses and is  
973 activated by bacterial DAP-type PGN. Our data demonstrated that pLB1+ neurons responded  
974 to DAP-type PGN in a dose-dependent manner and detected caffeine (a bitter compound for  
975 flies), but not sucrose, confirming their bitter nature (Fig. 2a, b, Movie 1, 2).

976 Considering that the pLB1<sup>Gal4</sup> transgene drives the expression of Gal4 in neurons other than  
977 GRNs and in immune cells, and that all pLB1+ GRNs are Gr66a+, we decided to study PGN  
978 perception by bitter gustatory neurons in the well-characterized Gr66a+ GRN population. As  
979 for labellar pLB1+ gustatory neurons, calcium imaging revealed that DAP-type PGN activates  
980 Gr66a+ neurons (Fig. 2c, d, Movie 3). Together, these results showed that bitter GRNs, among  
981 which some express the PGRP-LB protein, are able to respond to DAP-type PGN. Moreover,  
982 when we exposed flies to *E. coli*, a Gram-negative bacterium that produces DAP-type PGN and  
983 known to activate the NF- $\kappa$ B/IMD cascade in immune tissues, we also detected a response in  
984 Gr66a+ neurons, demonstrating that these neurons are able to directly detect bacteria (Fig. 2c,  
985 d). Because of the highly complex biochemical composition of bacteria, we decided for the next

986 experiments to focus on the sensing of pure PGN. To evaluate the specificity of this response,  
987 pLB1<sup>Gal4</sup>/UAS-GCaMP6s and Gr66a<sup>Gal4</sup>/UAS-GCaMP6s flies were exposed to Lys-type PGN,  
988 that does not interact with PGRP-LB and does not activate the NF- $\kappa$ B/IMD cascade<sup>26</sup>. When  
989 used at concentrations at which DAP-type PGN is active, Lys-type PGN was unable to trigger  
990 calcium increase in pLB1+, nor in GR66a+ neurons (Fig. 2e, f). These data indicate that bitter-  
991 sensing gustatory neurons are responsive to the DAP-type PGN found in the cell wall of Gram-  
992 negative bacteria.

993

### 994 **Upstream elements of the NF- $\kappa$ B/IMD pathway are required for the response of bitter** 995 **GRNs to PGN**

996 Since some GRNs respond to DAP-type PGN, we tested whether the canonical upstream PGN  
997 sensors and downstream NF- $\kappa$ B/IMD pathway components were necessary to transduce its sig-  
998 nal, as it is for immune competent cells. For that purpose, *in vivo* calcium imaging experiments  
999 in pLB1<sup>Gal4</sup>/UAS-GCaMP6s flies were performed in various NF- $\kappa$ B/IMD mutant background  
1000 flies. Two PGRP proteins function as upstream DAP-type PGN (hereafter simply PGN) recep-  
1001 tors: PGRP-LC and PGRP-LE (Fig. 3a). While caffeine response was unaffected in *PGRP-LC*  
1002 (*PGRP-LC<sup>E12</sup>*) and *PGRP-LE* (*PGRP-LE<sup>112</sup>*) mutants (Extended Data Fig. 3-1a), PGN ability  
1003 to activate pLB1+ neurons was completely abrogated in *PGRP-LC* mutants (Fig. 3b) and to a  
1004 lesser extent, decreased in *PGRP-LE* animals. In contrast, PGN sensing in pLB1+ neurons was  
1005 not modified in the *PGRP-LB* mutant background compared to control animals (Fig. 3b). When  
1006 we studied the PGN response in Gr66a<sup>Gal4</sup>/UAS-GCaMP6s flies, the loss of PGRP-LC was also  
1007 sufficient to abolish this response, indicating that this membrane-associated receptor is required  
1008 in bitter-sensing neurons to detect the PGN (Fig. 3c).

1009 Since previous reports demonstrated that elements of the NF- $\kappa$ B/IMD pathway are expressed  
1010 and functionally required in some neurons<sup>18,20</sup>, their implication in mediating the effect of PGN  
1011 was tested. While loss-of-function mutants for *Dredd* (*Dredd<sup>D55</sup>*) (Fig. 3a) were responding  
1012 normally to caffeine, a strong reduction of calcium signal in pLB1+ neurons was observed in  
1013 flies stimulated with PGN (Fig. 3 b, c and Extended Data Fig. 3-1a, c). The conserved ability  
1014 of *Dredd* mutants to detect caffeine demonstrated that their unresponsiveness to PGN was nei-  
1015 ther secondary to neuronal death nor to a loss of cell functionality. To ensure that the NF-  
1016  $\kappa$ B/IMD pathway was required cell-autonomously in gustatory neurons, we used RNAi-medi-  
1017 ated cell-specific inactivation. Functional downregulation of the *PGRP-LC*, *IMD*, *Fadd*, and  
1018 *Dredd* in GR66a+ cells, was sufficient to block calcium response after PGN stimulation (Fig.



1019 **3d**). These neurons remained responsive to caffeine (Extended Data **Fig. 3-1d**) demonstrating  
1020 that the NF- $\kappa$ B/IMD pathway upstream components inactivation specifically impaired the re-  
1021 sponse to PGN. Since most of the reported IMD-dependent responses have been shown to be  
1022 mediated by the NF- $\kappa$ B transcription factor Relish, we tested its implication in bitter GRNs  
1023 response to PGN<sup>9, 13</sup>. Intriguingly, the calcium response of Gr66a+ neurons upon proboscis  
1024 stimulation by PGN or caffeine was not statistically different in *Relish* RNAi flies compared to  
1025 wild-type controls (**Fig. 3d** and Extended Data **Fig. 3-1d**). Altogether, these data demonstrate  
1026 that Gr66a+ neurons can respond to DAP-type PGN in an IMD-pathway dependent manner,  
1027 but suggest that it is independent of the canonical Relish trans-activator.

1028

### 1029 **The response of bitter-sensing neurons to peptidoglycan does not require TrpA1 nor** 1030 **Gr66a**

1031 A previous work has shown that another ubiquitous component of the Gram-negative bacterial  
1032 cell wall, LPS, is detected in esophageal Gr66a+ bitter-sensing neurons via the TrpA1 cation  
1033 channel<sup>25</sup>. To assess whether TrpA1 is implicated in the response of neurons to PGN, we per-  
1034 formed *in vivo* calcium imaging in *dTrpA1* mutants. The fact that PGN-dependent activation of  
1035 cells is conserved in TrpA1 mutants demonstrated that PGN and LPS are detected by different  
1036 receptors and certainly trigger different pathways in bitter GRNs (Extended Data **Fig. 3-1b**).  
1037 The non-GPCR gustatory receptor GR66a itself was also not involved in mediating the response  
1038 to PGN. Altogether, these results suggest that PGRP-LC could be the dedicated receptor nec-  
1039 cessary for PGN detection and transduction in bitter-sensing neurons.

1040

### 1041 **Activation of the NF- $\kappa$ B/IMD pathway in bitter-sensing neurons modulate aversive be-** 1042 **haviors**

1043 The ability of PGN to activate calcium release in bitter GRNs prompted us to test whether PGN  
1044 triggers aversive behaviors in flies. We tested this hypothesis using the FlyPAD device in a  
1045 two-choice feeding assay (**Fig.4a**)<sup>39</sup>. When flies were given a choice between a sucrose only  
1046 and a sucrose plus PGN solution, no obvious repulsive behavior towards PGN was detected  
1047 (**Fig.4b** and Extended Data **Fig. 4-1a, b**). To further evaluate the phenotypical consequences  
1048 associated with activation of the NF- $\kappa$ B/IMD pathway specifically in the Gr66a+ neurons, we  
1049 overexpressed the upstream signaling receptor PGRP-LCa in these cells. This ectopic expres-  
1050 sion may hypersensitize the cells to PGN and has been shown to induce forced dimer receptor  
1051 formation and hence to trigger downstream signaling in the absence of the ligand or with lower

1052 amounts of it. In a two-choice feeding assay, flies in which PGRP-LCa was overexpressed in  
1053 GR66a<sup>+</sup> neurons, showed an increased repulsion towards solution containing PGN (Fig. 4c).  
1054 This behavior, which was not observed in control animals, was abolished by the simultaneous  
1055 knockdown of the NF- $\kappa$ B/IMD downstream element *Fadd* (Fig. 4d). Thus, when sensitized  
1056 following over-expression of the PGRP-LCa receptor, flies can discriminate, via the IMD path-  
1057 way between a sucrose containing PGN solution and a sucrose only solution. Since lactic acid  
1058 bacteria *Enterococci* are critical modulators to attract *Drosophila* to lay eggs on decaying food  
1059 <sup>40</sup>, we then tested whether IMD-dependent activation of bitter-sensing neurons would impact  
1060 egg-laying site preference. Although we were unable to detect any bias of egg-laying toward  
1061 PGN contaminated media (data not shown), we observed that PGRP-LCa overexpression in  
1062 Gr66a<sup>+</sup> neurons directly led to a decreased oviposition (Fig. 4e, f). This decreased egg-laying  
1063 when PGRP-LCa is expressed in bitter-sensing gustatory neurons was confirmed using  
1064 Gr32a<sup>Gal4</sup> as another bitter GRNs driver (Extended Data Fig. 4-1c). These results suggesting  
1065 that NF- $\kappa$ B/IMD pathway activation in bitter GRNs reduces female egg-laying were further  
1066 confirmed by showing that this effect could be suppressed by the simultaneous RNAi-mediated  
1067 *Fadd* inactivation in Gr66a<sup>+</sup> neurons (Fig. 4g). In contrast, simultaneous knockdown of the  
1068 transcription factor *Relish* did not impact the egg-laying decrease, indicating that this trans-  
1069 activator is not required for this PGN-mediated behavioral response (Fig. 4g). We previously  
1070 showed that PGN-dependent NF- $\kappa$ B/IMD pathway activation in a subset of brain octopamin-  
1071 ergic neurons was sufficient to reduce female egg-laying, a phenomenon reproduced with  
1072 Kir2.1 overexpression in these neurons, suggesting the PGN-dependent inactivation of this oc-  
1073 topaminergic neurons <sup>20</sup>. Importantly, inactivating the Gr66a<sup>+</sup> cells via Kir2.1 expression did  
1074 not phenocopy the egg-laying drop caused by inactivation of octopaminergic neurons, suggest-  
1075 ing that PGRP-LCa overexpression triggered activation of Gr66a<sup>+</sup> neurons instead (Extended  
1076 Data Fig. 4-1d). Consistently, conditional Gr66a<sup>+</sup> cells activation via TrpA1 overexpression,  
1077 that leads to inward current flux of cations, decreased female egg-laying (Fig. 4h). Taken to-  
1078 gether, these data demonstrate that receptor and transducers of the NF- $\kappa$ B/IMD pathway (but  
1079 not the downstream NF- $\kappa$ B transcription factor Relish) are expressed and functionally required  
1080 in bitter-sensing-neurons to mediate a behavioral response towards PGN.

1081

## 1082 **Discussion**

1083 This study demonstrates that some neurons of the gustatory system detect the peptidoglycan,  
1084 one of the main conserved and ubiquitous cell wall bacterial components. In bitter-sensing Gus-  
1085 tatory neurons, this detection is mainly mediated by the IMD pathway PGRP-LC receptor and

1086 thus probably not by classical Gr proteins such as Gr66a. The PGN signal is transduced by the  
1087 known cytosolic members of the IMD pathway such as Fadd and Dredd. Together with previous  
1088 reports, these results confirm the key role played by the PGRP/IMD module in regulating many  
1089 of the interactions between PGN and flies. This specific recognition step, which takes place at  
1090 the cell membrane via PGRP-LC or within the cells via PGRP-LE, has been shown to control  
1091 the production of anti-bacterial effectors by immune-competent cells, to alter the egg-laying  
1092 rate of infected females and to allow the physiological adaptation of the flies to their infectious  
1093 status<sup>18, 19, 20, 28, 41, 42, 43</sup>. Interestingly, while the initial MAMP/PRR recognition event is con-  
1094 served among these processes, the downstream molecular mechanisms that transduce the signal  
1095 are context-dependent. Whereas the PGN-dependent activation of an immune response in adi-  
1096 pocytes, hemocytes or enterocytes and the inhibition of VUM III octopaminergic brain neurons  
1097 rely on the nuclear NF- $\kappa$ B/Relish protein, the transcriptionally regulated effectors are likely to  
1098 be different<sup>10, 20</sup>. The response of bitter-sensing-neurons to PGN depends on a non-canonical  
1099 IMD pathway in which NF- $\kappa$ B/Relish is not required. Interestingly, PGRP-LC and some down-  
1100 stream IMD components are also required at the pre-synaptic terminal of *Drosophila* motoneu-  
1101 rons for robust presynaptic homeostatic plasticity<sup>44, 45</sup>. The local modulation of the presynaptic  
1102 vesicle release, which occurs in seconds following inhibition of postsynaptic glutamate recep-  
1103 tors, required PGRP-LC, Tak1 but is also Relish-independent. These data and ours raise im-  
1104 portant questions regarding how the activation of the upstream elements of the IMD cascade is  
1105 modifying neuronal activity, a topic for future studies. Previous biochemical studies have  
1106 shown that IMD signaling is rapid, occurring in seconds, a time frame consistent with its role  
1107 at the synapse and now in bitter-sensing neurons signal transduction<sup>46</sup>. Another possibility for  
1108 the involvement of the IMD pathway in the bitter-sensing neurons would be that the expression  
1109 of a yet to be identified PGN sensor requires the PGRP/IMD module for a permissive signal  
1110 upon stimulation by environmental bacteria.

1111 Our data show that flies can perceive PGN, a component of the bacteria cell wall, via bitter-  
1112 sensing neurons. These findings are complementary to observations made for another cell wall  
1113 component in Gram-negative bacteria, called LPS, which triggers feeding and oviposition  
1114 avoidance in *Drosophila* through the activation of bitter-sensing neurons<sup>25</sup>. While LPS induced  
1115 avoidance behavior is mediated through the canonical chemosensory cation channel TrpA1, we  
1116 show that PGN induced activation of bitter-sensing neurons seems to be independent of it. It  
1117 seems to be also independent of the classical Gr receptors but to depend on a dedicated PGN  
1118 sensor used in other contexts. We demonstrate that the bitter response upon PGN stimulation is  
1119 dependent on the IMD pathway that not only regulates a feeding aversion for PGN but also

1120 modulate oviposition rate. This indicates that PGN detection by gustatory neurons and its relay  
1121 by the IMD pathway is probably an informative environmental cue for flies. Our approach fo-  
1122 cusing on purified PGN allows us to directly link a molecule to the neurons and the molecules  
1123 that perceive it. However, the behavior of flies in a natural environment most probably corre-  
1124 sponds to a highly complex integration of multiple intricate signals perceived by different sen-  
1125 sory systems of the animal. For instance, lactic acid, which is produced by some bacteria is also  
1126 sensed by gustatory neurons<sup>47</sup>. In this respect, it remains difficult to appreciate to which con-  
1127 centrations of bacteria-derived products animal sensory system are exposed in their natural en-  
1128 vironment. Assays estimated the amount of LPS at the surface of fruits of around 1000µg/mL  
1129 <sup>25</sup>. To our knowledge, no such studies were performed for PGN. It should also be mentioned  
1130 that the amount of PGN released by bacteria is highly dependent on the species considered and  
1131 the bacterial growth phase to cite only few parameters <sup>48</sup>. The ability of the PGN to serve as a  
1132 ligand for its host receptor also depends on other cell wall component such as teichoic acid, but  
1133 also on PGN degrading enzymes such as amidase or lysozymes that degrade it<sup>49</sup>. It is therefore  
1134 complicated to speculate on what could be a physiological concentration of PGN for flies sens-  
1135 ing its environment.

1136 Thus, in nature, PGN is likely detected in combination with other tastants and odorants, which  
1137 detected alone may lead to an array of conflicting behaviors but in combination will yield in  
1138 one context-dependent behavioral output <sup>25, 50</sup>. Consequently, it may be hazardous to expect  
1139 clear phenotypes, or to make sense of the observed ones for the ecology of the fly when testing  
1140 a single molecule of the permanent environment of the animal while this molecule is not espe-  
1141 cially deleterious *per se*, but rather informative for the insect. The PGN is an interesting case  
1142 as on one hand, an internal sensing of this molecule indicates an infection, the uncontrolled  
1143 growth of a bacteria or a breach in a physical barrier. On the other hand, the perception of this  
1144 same molecule in the environment might be a clue, among others, to suggest a heavily contam-  
1145 inated place.

1146 **Figure legends**

1147

1148 **Figure 1. An IMD pathway component is expressed in neurons located in the proboscis.**

1149 Detection of cells expressing pLB1<sup>Gal4</sup>/UAS-mCD8-GFP (pLB1+). **a.** Schematic representing  
1150 the fly head and the axonal projections of pLB1+ peripheral neurons (green). The proboscis is  
1151 an appendix dedicated to the feeding process and hosting neurons dedicated to detection of  
1152 tastants. The cell bodies of pLB1+ neurons are located in labellar sensilla exposed to the envi-  
1153 ronment and project axons to the brain, specifically in the sub-esophageal zone (SEZ). **b.** In the  
1154 brain of female flies, labellar pLB1+ neurons project in the SEZ with a reproducible pattern  
1155 (n=25). The panel on the right is a magnification of the SEZ delineated by the white box. **c.** The  
1156 projections seen in the SEZ arise from neurons whose cell bodies are located in the tip of the  
1157 proboscis (Table 1, n=32), the labellum. The panel on the right is a magnification of the label-  
1158 lum delineated by the white box. **d, e.** Immunodetection in the brain (**d**) and detection in the  
1159 proboscis (**e**) of cells expressing pLB1<sup>Gal4</sup>/UAS-mCD8-GFP (pLB1+) as well as Gr66a-RFP  
1160 (Gr66a+) (n=5 for brains and 6 for proboscises). **d.** Top left is a view of a large portion of the  
1161 brain, the other panels are magnifications of the SEZ delineated by the white box. **d, e.** All the  
1162 pLB1+ projections and neurons (arrowheads) are Gr66a+ while not all the Gr66a+ projections  
1163 and cells (arrows) are pLB1+. Scale bar, 50  $\mu$ m. n indicates the number of examined brains or  
1164 proboscises. Stacks of images were analyzed. For the proboscises, sagittal views, anterior is on  
1165 the right with dorsal part and maxillary palps sometimes visible at the bottom. See also Table  
1166 1, Table 2, extended Data [Fig. 1-1](#) and [Fig 1-2](#).

1167

1168 **Figure 2. Bitter gustatory receptor neurons respond to DAP-type peptidoglycan.**

1169 Real-time calcium imaging using the calcium indicator GCaMP6s to assess the *in vivo* neuronal  
1170 activity in the sub-esophageal zone (SEZ) of labellar pLB1+ neurons (pLB1<sup>Gal4</sup>/UAS-  
1171 GCaMP6s) (**a, b**) or bitter gustatory receptor neurons (Gr66a<sup>Gal4</sup>/UAS-GCaMP6s) (**c, d**). **a** and  
1172 **c.** Representative images (top) and averaged fluorescence  $\pm$  SEM time course of the GCaMP6s  
1173 intensity variations ( $\Delta F/F_0\%$ ) (bottom). The addition of the chemical on the proboscis at a spe-  
1174 cific time is indicated by the arrow. **a.** The images illustrate the GCaMP6s intensity before and  
1175 after the addition of either water as negative control (left panels), peptidoglycan (PGN 100  
1176  $\mu$ g/mL; middle panels), caffeine or sucrose (right panels) on the proboscis. Scale bar, 20  $\mu$ m.  
1177 **c.** The images illustrate the GCaMP6s intensity before and after the addition of either water as  
1178 negative control, *E. coli* K12 (OD600=0.5), peptidoglycan (PGN; 100  $\mu$ g/mL), caffeine or su-  
1179 crose (from left to right panel) on the proboscis. Scale bar, 20  $\mu$ m. **b.** Averaged fluorescence

1180 intensity of peaks ( $\Delta F/F_0$ )  $\pm$  SD for control, PGN (different concentrations), caffeine or sucrose  
1181 stimulated flies (n= 7-8). **d.** Averaged fluorescence intensity of peaks  $\pm$  SD for control, *E. coli*  
1182 K12(OD600=0.5), PGN (100  $\mu$ g/mL), caffeine or sucrose stimulated flies (n=7-9). **e** and **f.** Av-  
1183 eraged fluorescence intensity of peaks ( $\Delta F/F_0$ )  $\pm$  SD for pLB1<sup>Gal4</sup>/UAS-GCaMP6s (n=7-8) (**e**)  
1184 or Gr66a<sup>Gal4</sup>/UAS-GCaMP6s (n=7-8) (**f**) flies exposed to water, Lys-type PGN (100  $\mu$ g/mL) or  
1185 DAP-type PGN (100  $\mu$ g/mL). n indicates the number of analyzed animals (single dots in  
1186 graphs) for each condition. \*\*\* indicates  $p < 0.0001$ ; non-parametric t-test, Mann-Whitney test.  
1187

1188 **Figure 3. The PGN detection in pLB1+and Gr66a+ neurons requires upstream elements**  
1189 **of the NF- $\kappa$ B/IMD pathway.**

1190 **a.** Schematic of the canonical NF- $\kappa$ B/IMD pathway in *Drosophila*. **b-d.** Real-time calcium im-  
1191 aging using the calcium indicator GCaMP6s to assess the *in vivo* neuronal activity in the sub-  
1192 esophageal zone (SEZ) of labellar pLB1+ neurons (pLB1<sup>Gal4</sup>/UAS-GCaMP6s) (**b**) or bitter gust-  
1193 atory receptor neurons (Gr66a<sup>Gal4</sup>/UAS-GCaMP6s) (**c,d**). **b, c.** Averaged fluorescence intensity  
1194 of peaks ( $\Delta F/F_0$ )  $\pm$  SD for pLB1<sup>Gal4</sup>/UAS-GCaMP6s (n=8-9). (**b**) or Gr66a<sup>Gal4</sup>/UAS-GCaMP6s  
1195 (n=7-8) (**c**) flies in different mutant backgrounds and exposed to PGN (100  $\mu$ g/mL). **d.** Aver-  
1196 aged fluorescence intensity of peaks ( $\Delta F/F_0$ )  $\pm$  SD for Gr66a<sup>Gal4</sup>/UAS-GCaMP6s animals ex-  
1197 pressing RNAi targeting different elements of the NF- $\kappa$ B/IMD pathway and exposed to PGN  
1198 (100  $\mu$ g/mL) (n= 6-8). n indicates the number of analyzed animals (single dots in graphs) for  
1199 each condition. \*\*\* indicates  $p < 0.0001$ ; non-parametric t-test, Mann-Whitney test. See also  
1200 extended Data [Fig. 3-1](#).  
1201

1202 **Figure 4. Over-expression of the PGN receptor PGRP-LCa in bitter-sensing neurons**  
1203 **modulates feeding preference towards peptidoglycan and oviposition behavior.**

1204 **a.** Schematic of the two-choice feeding assay using the flyPAD device<sup>39</sup>. Individual flies are  
1205 given the choice between a sucrose solution (5mM) and a sucrose solution (5mM) plus pepti-  
1206 doglycan (PGN) and tested for 1 hour. **b-d.** Feeding preference is expressed as a Preference  
1207 Index (PI) based on the number of sips (see **Material and Methods**). **b.** Feeding preference of  
1208 wild type (*Canton S*) flies exposed to two sucrose solutions (5mM), one of which containing  
1209 PGN (different concentrations are tested and indicated in the X axis) (n=50-68). **c.** Feeding  
1210 preference of flies overexpressing PGRP-LCa in bitter taste neurons (Gr66a<sup>Gal4</sup>/UAS-PGRP-  
1211 LCa) and controls exposed to two sucrose solutions (5mM), one of which containing PGN (100  
1212  $\mu$ g/mL) (n= 61-73). **d.** Feeding preference of flies overexpressing simultaneously PGRP-LCa

1213 and UAS Fadd RNAi in bitter taste neurons ( $Gr66a^{Gal4}/UAS-PGRP-LCa$ , UAS-Fadd RNAi)  
1214 and control animals exposed to two sucrose solutions (5mM), one of which containing PGN  
1215 (100  $\mu\text{g}/\text{mL}$ ) (n=49-52). **e.** Schematic of the oviposition assay. Individual flies are transferred  
1216 in fresh tubes and allowed to lay eggs for 24 hours (24h). **f.** Eggs laid per 24h by flies overex-  
1217 pressing PGRP-LCa in bitter taste neurons ( $Gr66a^{Gal4}/UAS-PGRP-LCa$ ) and control animals  
1218 (n=80-92). **g.** Eggs laid per 24h by flies overexpressing simultaneously PGRP-LCa and Fadd  
1219 RNAi or Relish RNAi in bitter-sensing gustatory neurons ( $Gr66^{Gal4}/UAS-PGRP-LCa$ , UAS-  
1220 Fadd RNAi) and control animals (n=24-76). **h.** Eggs laid per 24h by flies overexpressing TrpA1  
1221 in bittersensing neurons ( $Gr66^{Gal4}/UAS-TrpA1$ ) and control animals, at a permissive (23°C)  
1222 and restrictive (29°C) temperature (n=18-20). **b-d.** shown are the average  $PI \pm SD$  of at least  
1223 three independent trials. \*\*\* indicates  $p < 0.0001$ ; ns indicates  $p > 0.05$ ; non-parametric t-test,  
1224 Mann-Whitney test. **f-h.** shown are the average numbers of eggs laid per fly per 24 h  $\pm SD$  from  
1225 at least two independent trials with at least 20 females per trial, genotype and condition used.  
1226 \*\*\* indicates  $p < 0.0001$ ; ns indicates  $p > 0.05$ ; non-parametric ANOVA, Dunn's multiple com-  
1227 parison test. n indicates number of analyzed animals (single dots in graphs) for each condition.  
1228 See also extended Data [Fig. 4-1](#).

1229

## 1230 **Extended data**

1231

### 1232 **Figure 1-1. pLB2 and pLB3 expressions are not detected in the fly labellum.**

1233 **a.** Schematic representation showing the PGRP-LB locus (adapted from FlyBase <http://fly->  
1234 [base.org/reports/FBgn0037906.html](http://fly-base.org/reports/FBgn0037906.html) and from <sup>18</sup>. The exonic coding sequences are indicated in  
1235 light purple, while the non-coding exonic sequence in dark purple. In green are represented the  
1236 fragments used to generate the  $pLB1^{Gal4}$ ,  $pLB2^{Gal4}$  and  $pLB3^{Gal4}$  constructs <sup>18</sup>. **b.** Detection in  
1237 the labella of  $pLB1+$  ( $pLB1^{Gal4}/UAS-mCD8-GFP$ ; n=32),  $pLB2+$  ( $pLB2^{Gal4}/UAS-mCD8-GFP$ ;  
1238 n=7) and  $pLB3+$  ( $pLB3^{Gal4}/UAS-mCD8-GFP$ ; n=3) cells (from left to right, respectively).  
1239 Stacks of images were analyzed.

1240

### 1241 **Figure 1-2. pLB1+ neurons in the labellum are exclusively Gr66a+.**

1242 **a.** Immunodetection in brain (top) and detection in the proboscis (bottom) of cells  $pLB1+$  as  
1243 well as  $Gr66a+$  via genetic intersectional strategy ( $pLB1^{Gal4}$ ,  $Gr66a^{LexA}/UASfritSTOPfritmCD8-$   
1244  $GFP$ ,  $LexAopFLP$ ; n=5 brains and n=4 proboscices). Arrows point to  $pLB1+/Gr66a+$  cellular  
1245 bodies. **b.** Immunodetection in brain (top) and detection in the proboscis (bottom) of cells  
1246  $pLB1+$  and  $Gr66a-$  ( $pLB1+/Gr66a-$ ) via the expression of the Gal4 inhibitor Gal80 specifically

1247 in Gr66a<sup>+</sup> cells (pLB1<sup>Gal4</sup>; UAS-mCD8-GFP/Gr66a<sup>LexA</sup>, LexAopGal80; n=3 brains and n=4  
1248 proboscises). **c.** Immunodetection in the brain of cells pLB1<sup>+</sup> as well as Gr32a<sup>+</sup> via genetic  
1249 intersectional strategy (pLB1<sup>Gal4</sup>/Gr32a<sup>LexA</sup>; UAS*firt*STOP*firt*mCD8GFP, LexAopFLP; n=3). **d.**  
1250 Immunodetection in the brain of cells pLB1<sup>+</sup> as well as Gr5a<sup>+</sup> via genetic intersectional strat-  
1251 egy (pLB1<sup>Gal4</sup>, Gr5a<sup>LexA</sup>/UAS*firt*STOP*firt*mCD8GFP, LexAopFLP; n=2). **e.** Detection in the  
1252 proboscis of cells producing the endogenous PGRP-LB (PGRP-LB::GFP) as well as Gr66a-  
1253 RFP (Gr66a<sup>+</sup>). All the PGRP-LB::GFP<sup>+</sup> cells (arrowheads) are Gr66a<sup>+</sup> while not all the  
1254 Gr66a<sup>+</sup> cells (arrows) are PGRP-LB::GFP<sup>+</sup> (n=4). In **a-d**, the right panels are magnifications  
1255 of the sub-esophageal zone delineated by the white box. All the images of the proboscis are  
1256 sagittal views with anterior on the right and dorsal at the bottom. n indicates number of exam-  
1257 ined brains or proboscises. Scale bar, 50  $\mu$ m.

1258

1259 **Figure 3-1. The NF- $\kappa$ B/IMD pathway is not required for bitter -sensing gustatory neurons**  
1260 **response to caffeine and pLB1<sup>+</sup> neurons response to PGN does not necessitate Gr66a or**  
1261 **dTrpA1.**

1262 Real-time calcium imaging using the calcium indicator GCaMP6s to assess the *in vivo* neuronal  
1263 activity in the SEZ of pLB1<sup>+</sup> (**a** and **b**) or Gr66a<sup>+</sup> (**c** and **d**) neurons. **a,c.** Averaged fluorescence  
1264 intensity of peaks ( $\Delta F/F_0$ )  $\pm$  SD for pLB1<sup>Gal4</sup>/UAS-GCaMP6s (n=6-7) (**a**) or Gr66a<sup>Gal4</sup>/UAS-  
1265 GCaMP6s (n=7-8) (**c**) flies in different mutant backgrounds exposed to caffeine (10mM). **b.**  
1266 Averaged fluorescence intensity of peaks  $\pm$  SD for pLB1<sup>Gal4</sup>/UAS-GCaMP6s flies in different  
1267 mutant backgrounds exposed to peptidoglycan (100  $\mu$ g/mL) (n=6-8). **d.** Averaged fluorescence  
1268 intensity of peaks  $\pm$  SD for Gr66a<sup>Gal4</sup>/UAS-GCaMP6s animals expressing RNAi against IMD  
1269 pathway elements and exposed to caffeine (10mM) (n=7-8). n indicates the number of analyzed  
1270 animals (single dots in graphs) for each condition. ns indicates  $p > 0.05$ ; non-parametric t-test,  
1271 Mann-Whitney test.

1272

1273 **Figure 4-1. While PGN is neither attractive nor aversive for wild type flies in two-choice**  
1274 **feeding assay, IMD pathway activation in bitter-sensing neurons inhibits egg laying.**

1275 **a,b.** Feeding preference of *yw* (n=82-99) (**a**) or *w* (n=50-63) (**b**) flies exposed to two sucrose  
1276 solutions (5mM), one of which containing PGN (different concentrations are tested and indi-  
1277 cated in the X axis). **c** Eggs laid per 24 hours (24h) by flies overexpressing PGRP-LCa in bitter-  
1278 sensing gustatory neurons (Gr32a<sup>Gal4</sup>/UAS- PGRP-LCa) and control animals (n=60). **d.** Eggs  
1279 laid per 24 hours (24h) by flies overexpressing kir2.1 in bitter taste neurons (Gr66a<sup>Gal4</sup>/UAS-  
1280 kir2.1) and control animals (n=60). **a,b.** Shown are the average Preference Index (PI)  $\pm$  SD of



1281 at least 5 independent trials. \*\*\* indicates  $p < 0.0001$ ; ns indicates  $p > 0.05$ ; non-parametric t-  
1282 test, Mann-Whitney test. **c,d.** Shown are the average numbers of eggs laid per fly per 24 h  $\pm$  SD  
1283 from at least two independent trials with at least 20 females per trial, genotype and condition  
1284 used. \*\*\* indicates  $p < 0.0001$ ; ns indicates  $p > 0.05$ ; non-parametric ANOVA, Dunn's multiple  
1285 comparison test. n indicates the number of analyzed animals (single dots in graphs) for each  
1286 condition.

1287

1288 **Table 1. Number of GFP-positive neurons for labellum in pLB1<sup>Gal4</sup>/UAS-mCD8-GFP**  
1289 **flies.**

1290 The amount of times (N) a precise quantity of pLB1+ neurons is detected (event) is shown over  
1291 the total amount of proboscises observed. Only 1-week old female flies were analyzed.

1292 **Table 2. Number of cells pLB1+ as well as Gr66a+ in labellum of pLB1<sup>Gal4</sup>, UAS-mCD8-**  
1293 **GFP/Gr66a-RFP 1-week old female flies.**

1294 The amount of pLB1+ neurons, Gr66a+ neurons and co-stained cells are presented.

1295

1296 **Movie 1. pLB1+ neurons respond *in vivo* to PGN.**

1297 Real-time calcium imaging using the calcium indicator GCaMP6s to assess the *in vivo* neuronal  
1298 activity in the sub-esophageal zone of pLB1 neurons (pLB1<sup>Gal4</sup>/UAS-GCaMP6s). Effect of pep-  
1299 tidoglycan solution stimulation (100  $\mu$ g/mL) on the proboscis. GFP signal was recorded every  
1300 500 ms and the PGN was added at 1 second after the beginning of the recording.

1301

1302 **Movie 2. pLB1+ neurons respond *in vivo* to caffeine.**

1303 Real-time calcium imaging using the calcium indicator GCaMP6s to assess the *in vivo* neuronal  
1304 activity in the sub-esophageal zone of pLB1 neurons (pLB1<sup>Gal4</sup>/UAS-GCaMP6s). Effect of caf-  
1305 feine solution stimulation (10 mM) on the proboscis. GFP signal was recorded every 500 ms  
1306 and the caffeine was added at 1 second after the beginning of the recording

1307

1308 **Movie 3. Gr66a+ neurons respond *in vivo* to PGN.**

1309 Real-time calcium imaging using the calcium indicator GCaMP6s to assess the *in vivo* neuronal  
1310 activity in the sub-esophageal zone of bitter-sensing neurons (Gr66a<sup>Gal4</sup>/UAS-GCaMP6s). Ef-  
1311 fect of peptidoglycan solution stimulation (100  $\mu$ g/mL). GFP signal was recorded every 500  
1312 ms and the PGN was added at 1 second after the beginning of the recording.

1313

1314 **Methods**

1315 **Experimental designs**

1316

1317 **Fly stocks**

1318 Detailed genotypes of all the flies used can be found in the **supplementary raw data** under-  
1319 lying the results.

1320 All flies were maintained at 25°C on a standard cornmeal/agar medium on a 12 h:12 h light-  
1321 dark cycle with a relative humidity of 70%. The strains used are the following: pLB1<sup>Gal4</sup> 18;  
1322 PGRP-LB::GFP 20; w (BDSC:3605); yw ; Canton-S; Gr5a<sup>LexA</sup> 51, 52 (Gently provided by Dong  
1323 Min Shin); Gr66a<sup>LexA</sup> (53; gently provided by K. Scott's Lab); Gr32a<sup>LexA</sup> 54 (gently provided by  
1324 A. Dahanukar's lab); Gr32a<sup>Gal4</sup> (BDSC:57622); Gr66a<sup>Gal4</sup> ; Gr66a-RFP(X4) (BDSC:60691);  
1325 UAS-TrpA1 (BDSC:26264,55); UAS-Kir2.1 (BDSC:6595); 40XUAS-mCD8-GFP  
1326 (BDSC:32195); UAS-Fadd RNAi<sup>56</sup>; UAS-Imd RNAi (VDRC#101834) ; UAS-Dredd-RNAi  
1327 (VDRC#104726); UAS-PGRP-LC RNAi (VDRC#101636); UAS-Relish RNAi  
1328 (BDSC:28943); UAS<sup>frit</sup>STOP<sup>frit</sup> mCD8GFP (BDSC:30125); 8XLexAop2-FLP  
1329 (BDSC:55819); UAS-GCaMP6s (BDSC:42746). UAS-PGRP-LCa 57; PGRP-LC<sup>E12</sup> 58; PGRP-  
1330 LE<sup>112</sup> 59 ; PGRP-LB<sup>ko</sup> 60 ; Dredd<sup>D55</sup> 61; TrpA1<sup>1</sup> 25.

1331 **Tastants**

1332 For *in vivo* calcium imaging and flyPAD assays tastants were dissolved in autoclaved purified  
1333 distilled water. All tastant solutions were freshly prepared and stored in aliquots at -20°C for a  
1334 maximum duration of six months. Peptidoglycan was obtained from InvivoGen (PGN-EK Cat-  
1335 alog # tlr-pgnek, InvivoGen, USA), while sucrose (Roth, ref 4621.1) and caffeine (Sigma Al-  
1336 drich, ref C0750) were obtained from Sigma-Aldrich (USA).

1337 ***In vivo* calcium imaging**

1338 *In vivo* calcium imaging experiments were performed on 5-7 day-old starved mated females.  
1339 Animals were raised on conventional media with males at 25°C ~~or 29°C for RNAi experiments~~.  
1340 Flies were starved for 20-24 h in a tube containing a filter soaked in water prior any experi-  
1341 ments. Flies of the appropriate genotype were anesthetized on ice for 1 h. Female flies were  
1342 suspended by the neck on a plexiglass block (2 x 2 x 2.5 cm), with the proboscis facing the  
1343 center of the block. Flies were immobilized using an insect pin (0.1 mm diameter) placed on  
1344 the neck. The ends of the pin were fixed on the block with beeswax (Deiberit 502, Siladent,  
1345 209212). The head was then glued on the block with a drop of rosin (Gum rosin, Sigma-Aldrich  
1346 -60895-, dissolved in ethanol at 70 %) to avoid any movements. The anterior part of the head  
1347 was thus oriented towards the objective of the microscope. Flies were placed in a humidified  
1348 box for 1 h to allow the rosin to harden without damaging the living tissues. A plastic coverslip

1349 with a hole corresponding to the width of the space between the two eyes was placed on top of  
1350 the head and fixed on the block with beeswax. The plastic coverslip was sealed on the cuticle  
1351 with two-component silicon (Kwik-Sil, World Precision Instruments) leaving the proboscis ex-  
1352 posed to the air. Ringer's saline (130 mM NaCl, 5 mM KCl, 2 mM MgCl<sub>2</sub>, 2 mM CaCl<sub>2</sub>, 36  
1353 mM saccharose, 5 mM HEPES, pH 7.3) was placed on the head<sup>62</sup>. The antenna area, air sacs,  
1354 and the fat body were removed. The gut was cut without damaging the brain and taste nerves  
1355 to allow visual access to the anterior ventral part of the sub-esophageal zone. The exposed brain  
1356 was rinsed twice with Ringer's saline. GCaMP6s fluorescence was viewed with a Leica  
1357 DM600B microscope under a 25x water objective. GCaMP6s was excited using a Lumencor  
1358 diode light source at 482 nm ± 25. Emitted light was collected through a 505-530 nm band-pass  
1359 filter. Images were collected every 500 ms using a Hamamatsu/HPF-ORCA Flash 4.0 camera  
1360 and processed using Leica MM AF 2.2.9. Stimulation was performed by applying 140 µL of  
1361 tastant solution diluted in water on the proboscis. For *E. coli* K12 stimulation, bacteria were  
1362 grown in LB media overnight at 37°C, spined down 10 minutes at 3500g and the pellet sus-  
1363 pended in water to obtain a final OD600 of 0.5. A minimum of 2 independent experiments with  
1364 a total n for each condition ranging from 7 to 10 were performed. Each experiment consisted  
1365 of a recording of 10 images before stimulation and 30 images after stimulation. Data were an-  
1366 alyzed as previously described by using FIJI (<https://fiji.sc/>)<sup>62</sup>. In all experiments implicating  
1367 pLB1<sup>Gal4</sup>, this driver and the UAS-GCaMP6s transgenes are homozygous. In experiments using  
1368 Gr66a<sup>Gal4</sup>, the driver and the UAS-GCaMP6s transgenes are **heterozygous**.

### 1369 **Immunostaining and imaging**

1370 Immunostaining and imaging were performed as previously described<sup>20</sup>. Brains from adult fe-  
1371 males were dissected in Phosphate-buffered saline (PBS, Eurobio, ref CS0PBS0108) and fixed  
1372 for 15 min in 4% paraformaldehyde (Electron Microscopy Sciences, Cat # 15714-S) at room  
1373 temperature (RT). Afterward, brains were washed three times for 10 min in PBS-T (PBS +  
1374 0.3% Triton X-100) and blocked in 2,5% bovine serum albumin (BSA; Sigma-Aldrich) in PBS-  
1375 T for 30 min. After saturation, samples were incubated with the primary antibody diluted in  
1376 0,5% BSA in PBS-T overnight at 4°C. The following day, brains were washed three times and  
1377 incubated with the secondary antibody diluted in 0,5% BSA in PBS-T for 2 h at RT. Next,  
1378 samples were washed for 10 min in PBS-T and mounted on slides using Vectashield (Vector  
1379 Laboratories, Ca, USA) fluorescent mounting medium. In the case of proboscises, no im-  
1380 munostaining was performed. Proboscises of adult females were dissected in PBS, rinsed with  
1381 PBS and directly mounted on slides using Vectashield fluorescent mounting medium. The tis-  
1382 sues were visualized directly after.

1383 For the immunostaining the primary antibodies used are the following: Chicken anti-GFP (Aves  
1384 Labs Cat#GFP-1020, RRID:AB\_10000240. Dilution 1:1000), rabbit anti-RFP (Rockland  
1385 Cat#600-401-379, RRID:AB\_2209751. Dilution 1:1000), mouse anti-NC82 (DSHB  
1386 Cat#nc82,RRID:AB\_2314866. Dilution 1:40). The secondary antibodies used are the follow-  
1387 ing: Alexa Fluor 488 Donkey anti-Chicken IgY (IgG) (H+L) (Jackson ImmunoResearch Labs  
1388 Cat#703-545-155, RRID:AB\_2340375. Dilution 1:500), Alexa Fluor568 donkey anti-mouse  
1389 IgG (H+L) (Thermo Fisher Scientific Cat#A10037, RRID:AB\_2534013. Dilution 1:500),  
1390 Alexa Fluor647 donkey anti-mouse IgG (H+L) (Jackson ImmunoResearch Labs Cat#715-605-  
1391 151, RRID:AB\_2340863. Dilution 1:500), Alexa Fluor 568 donkey anti-rabbit IgG (H+L)  
1392 (Thermo Fisher Scientific Cat#A10042, RRID: AB2534017. Dilution 1:500).

1393 Images were captured with either a Leica SP8 confocal microscope (in this case, tissues were  
1394 scanned with 20X oil immersion objective) or an LSM 780 Zeiss confocal microscope (20x air  
1395 objective was used). For the detection of endogenous PGRP-LB::GFP, images were captured  
1396 with a Spinning Disk Ropper 2 Cam (20x or 40x air objective were used). Images were pro-  
1397 cessed using Adobe Photoshop.

#### 1398 **Feeding assay**

1399 5-7 day-old mated females were used. Animals were starved as a group for 20 h at 25°C prior  
1400 to the assay in a tube containing a filter soaked in water. Previously, these females were raised  
1401 with males on a conventional media at 25°C or 29°C for RNAi experiments. The assay could  
1402 not last more than 1 h as the food is totally consumed after this period. Two-choice feeding  
1403 assays were performed by using the flyPAD device<sup>39</sup> which records the cumulative number of  
1404 sips. Each sip corresponds to a contact of flies' proboscis with the chosen food substrate. Indi-  
1405 vidual flies were captured via aspiration (neither CO<sup>2</sup> nor ice used) and deposited in arenas  
1406 containing two food substrates. The control substrate consisted in a 1% agarose 5mM sucrose  
1407 solution, whereas the test substrate additionally contained peptidoglycan dissolved in water at  
1408 the indicated concentrations. Each arena's well (2 per arena) was filled with 3.5 µL of food  
1409 solution. Tests were run for 1 h at 25 °C under constant light in a behavioral room limiting the  
1410 influence of external light and noise. Data were collected and analyzed by using Bonsai<sup>63</sup> and  
1411 MATLAB, respectively (scripts provided by Pavel Itskov). Preference index was calculated as  
1412 following: (number of sips in the test solution - number of sips in the control solution)/ total  
1413 number of sips. Non eaters were excluded from the analysis.

#### 1414 **Oviposition assay**

1415 Oviposition assays were performed as previously described<sup>20</sup>. 5 day-old mated females were  
1416 used and raised on conventional media with males. Eclosed flies were raised at 25°C or 21°C,  
1417 in case of experiments involving the thermosensitive transgene UAS-TrpA1 or 29°C for RNAi  
1418 experiments. 5 day-old mated females were anesthetized on a CO<sub>2</sub> pad and singularly trans-  
1419 ferred in tubes containing a fresh (not older than 48h) conventional media with some dry yeast  
1420 (Fermipan) on top of it right before the egg-lay period. Flies were let to lay eggs for 24 h at  
1421 25°C or 23°C in control conditions for experiments involving UAS-TrpA1 or 29°C for test con-  
1422 ditions for experiments involving UAS-TrpA1 and RNAi experiments. After the egg-lay pe-  
1423 riod, animals were discarded and eggs were counted using a binocular scope. At least two in-  
1424 dependent trials with at least 20 females per trial, genotype and condition were used.

#### 1425 **Statistical analysis**

1426 Detailed statistical analyses and population sizes can be found in the **supplementary raw data**  
1427 underlying the results.

#### 1428 ***In vivo* calcium imaging**

1429 D'Agostino & Pearson test to assay whether the values are distributed normally was applied.  
1430 As not all the datasets were considered as normal, non-parametrical statistical analysis such as  
1431 non-parametric unpaired Mann-Whitney two-tailed tests or non-parametric unpaired ANOVA,  
1432 Kruskal-Wallis test, and Dunn's post-test were used for all the data presented.

#### 1433 **Feeding assay**

1434 D'Agostino & Pearson test to assay whether the values are distributed normally was applied.  
1435 As not all the datasets were considered as normal, non-parametrical statistical analysis such as  
1436 non-parametric unpaired Mann-Whitney two-tailed tests or non-parametric unpaired ANOVA,  
1437 Kruskal-Wallis test, and Dunn's post-test were used for all the data presented.

#### 1438 **Oviposition assay**

1439 D'Agostino & Pearson test to assay whether the values are distributed normally was applied.  
1440 As not all the datasets were considered as normal, non-parametrical statistical analysis and spe-  
1441 cifically the non-parametric unpaired ANOVA, Kruskal-Wallis test, and Dunn's post-test were  
1442 used for all the data presented.

1443

1444 GraphPad Prism 8 software was used for statistical analyses. For *in vivo* calcium imaging and  
1445 feeding assay analysis non-parametric unpaired Mann-Whitney two-tailed tests were

1446 performed. In the case of oviposition assay, we used the non-parametric unpaired ANOVA,  
1447 Kruskal-Wallis test, and Dunn's post-test.  
1448  
1449  
1450

1451

1452

1453 **Acknowledgments**

1454 We thank Emilie Avazeri and Annelise Viallat-Lieutaud for technical help. We thank members  
1455 of the Royet's laboratory for their comments on the manuscript. This work was supported by  
1456 (ANR-11-LABX-0054) (Investissements d'Avenir–Labex INFORM), ANR BACNEURODRO  
1457 (ANR-17-CE16-0023-01) and ANR PEPTIMET (ANR-18-CE15-0018-02), Equipe Fondation  
1458 pour la Recherche Médicale (EQU201903007783) and l'Institut Universitaire de France to J.R.  
1459 Y.G. laboratory is supported by the “Centre National de la Recherche Scientifique”, the “Uni-  
1460 versité de Bourgogne Franche-Comté”, the Conseil Régional Bourgogne Franche-Comte  
1461 (PARI grant), the FEDER (European Funding for Regional Economical Development), and the  
1462 European Council (ERC starting grant, GliSFCo-311403).

1463

1464 **Author contributions**

1465 Genetic epistasis and imaging and behavioral assay were performed by A.M. and L.K. Calcium  
1466 imaging was performed by G.M. Results were analyzed and interpreted by A.M., G.M., Y. G.,  
1467 L. K., and J. R. The original draft was written by J.R. Reviewing and editing were performed  
1468 by all authors. Supervision: L.K., Y.G., and J.R. Funding acquisition: Y.G, and J.R.

1469

1470

1471 **References**

1472

1473 1. Kavaliers, M., Ossenkopp, K.P. & Choleris, E. Pathogens, odors, and disgust in  
1474 rodents. *Neurosci Biobehav Rev* **119**, 281-293 (2020).

1475

1476 2. Sullivan, K., Fairn, E. & Adamo, S.A. Sickness behaviour in the cricket *Gryllus texensis*:  
1477 Comparison with animals across phyla. *Behav Processes* **128**, 134-143 (2016).

1478

1479 3. Mburu, D.M. *et al.* Relationship between virulence and repellency of  
1480 entomopathogenic isolates of *Metarhizium anisopliae* and *Beauveria bassiana* to the  
1481 termite *Macrotermes michaelseni*. *J Insect Physiol* **55**, 774-780 (2009).

1482

1483 4. Swanson, J.A. *et al.* Odorants that induce hygienic behavior in honeybees:  
1484 identification of volatile compounds in chalkbrood-infected honeybee larvae. *J Chem*  
1485 *Ecol* **35**, 1108-1116 (2009).

1486

1487 5. Hoffman, C. & Aballay, A. Role of neurons in the control of immune defense. *Curr*  
1488 *Opin Immunol* **60**, 30-36 (2019).

1489

1490 6. Aranha, M.M. & Vasconcelos, M.L. Deciphering *Drosophila* female innate behaviors.  
1491 *Curr Opin Neurobiol* **52**, 139-148 (2018).

1492



- 1493 7. Sayin, S., Boehm, A.C., Kobler, J.M., De Backer, J.F. & Grunwald Kadow, I.C. Internal  
1494 State Dependent Odor Processing and Perception-The Role of Neuromodulation in  
1495 the Fly Olfactory System. *Front Cell Neurosci* **12**, 11 (2018).  
1496
- 1497 8. Masuzzo, A., Montanari, M., Kurz, L. & Royet, J. How Bacteria Impact Host Nervous  
1498 System and Behaviors: Lessons from Flies and Worms. *Trends Neurosci* **43**, 998-1010  
1499 (2020).  
1500
- 1501 9. Zhai, Z., Huang, X. & Yin, Y. Beyond immunity: The Imd pathway as a coordinator of  
1502 host defense, organismal physiology and behavior. *Dev Comp Immunol* **83**, 51-59  
1503 (2018).  
1504
- 1505 10. Buchon, N., Silverman, N. & Cherry, S. Immunity in *Drosophila melanogaster*--from  
1506 microbial recognition to whole-organism physiology. *Nat Rev Immunol* **14**, 796-810  
1507 (2014).  
1508
- 1509 11. Martino, M.E., Ma, D. & Leulier, F. Microbial influence on *Drosophila* biology. *Curr*  
1510 *Opin Microbiol* **38**, 165-170 (2017).  
1511
- 1512 12. You, H., Lee, W.J. & Lee, W.J. Homeostasis between gut-associated microorganisms  
1513 and the immune system in *Drosophila*. *Curr Opin Immunol* **30**, 48-53 (2014).  
1514
- 1515 13. Myllymaki, H., Valanne, S. & Ramet, M. The *Drosophila* imd signaling pathway. *J*  
1516 *Immunol* **192**, 3455-3462 (2014).  
1517
- 1518 14. Lindsay, S.A. & Wasserman, S.A. Conventional and non-conventional *Drosophila* Toll  
1519 signaling. *Dev Comp Immunol* **42**, 16-24 (2014).  
1520
- 1521 15. De Gregorio, E., Spellman, P.T., Tzou, P., Rubin, G.M. & Lemaitre, B. The Toll and Imd  
1522 pathways are the major regulators of the immune response in *Drosophila*. *EMBO J*  
1523 **21**, 2568-2579 (2002).  
1524
- 1525 16. Royet, J., Gupta, D. & Dziarski, R. Peptidoglycan recognition proteins: modulators of  
1526 the microbiome and inflammation. *Nat Rev Immunol* **11**, 837-851 (2011).  
1527
- 1528 17. Kurata, S. Peptidoglycan recognition proteins in *Drosophila* immunity. *Dev Comp*  
1529 *Immunol* **42**, 36-41 (2014).  
1530
- 1531 18. Kurz, C.L., Charroux, B., Chaduli, D., Viallat-Lieutaud, A. & Royet, J. Peptidoglycan  
1532 sensing by octopaminergic neurons modulates *Drosophila* oviposition. *Elife* **6** (2017).  
1533
- 1534 19. Kobler, J.M., Rodriguez Jimenez, F.J., Petcu, I. & Grunwald Kadow, I.C. Immune  
1535 Receptor Signaling and the Mushroom Body Mediate Post-ingestion Pathogen  
1536 Avoidance. *Curr Biol* **30**, 4693-4709 e4693 (2020).  
1537
- 1538 20. Masuzzo, A. *et al.* Peptidoglycan-dependent NF-kappaB activation in a small subset of  
1539 brain octopaminergic neurons controls female oviposition. *Elife* **8** (2019).

1540

1541 21. Stensmyr, M.C. *et al.* A conserved dedicated olfactory circuit for detecting harmful

1542 microbes in *Drosophila*. *Cell* **151**, 1345-1357 (2012).

1543

1544 22. Min, S., Ai, M., Shin, S.A. & Suh, G.S. Dedicated olfactory neurons mediating

1545 attraction behavior to ammonia and amines in *Drosophila*. *Proc Natl Acad Sci U S A*

1546 **110**, E1321-1329 (2013).

1547

1548 23. Depetris-Chauvin, A., Galagovsky, D., Chevalier, C., Maniere, G. & Grosjean, Y.

1549 Olfactory detection of a bacterial short-chain fatty acid acts as an orexigenic signal in

1550 *Drosophila melanogaster* larvae. *Sci Rep* **7**, 14230 (2017).

1551

1552 24. Yanagawa, A., Neyen, C., Lemaitre, B. & Marion-Poll, F. The gram-negative sensing

1553 receptor PGRP-LC contributes to grooming induction in *Drosophila*. *PLoS One* **12**,

1554 e0185370 (2017).

1555

1556 25. Soldano, A. *et al.* Gustatory-mediated avoidance of bacterial lipopolysaccharides via

1557 TRPA1 activation in *Drosophila*. *Elife* **5** (2016).

1558

1559 26. Leulier, F. *et al.* The *Drosophila* immune system detects bacteria through specific

1560 peptidoglycan recognition. *Nat Immunol* **4**, 478-484 (2003).

1561

1562 27. Kaneko, T. *et al.* PGRP-LC and PGRP-LE have essential yet distinct functions in the

1563 *Drosophila* immune response to monomeric DAP-type peptidoglycan. *Nat Immunol* **7**,

1564 715-723 (2006).

1565

1566 28. Charroux, B. *et al.* Cytosolic and Secreted Peptidoglycan-Degrading Enzymes in

1567 *Drosophila* Respectively Control Local and Systemic Immune Responses to

1568 Microbiota. *Cell Host Microbe* **23**, 215-228 e214 (2018).

1569

1570 29. Lee, K.Z. & Ferrandon, D. Negative regulation of immune responses on the fly. *EMBO*

1571 *J* **30**, 988-990 (2011).

1572

1573 30. Chen, Y.D. & Dahanukar, A. Recent advances in the genetic basis of taste detection in

1574 *Drosophila*. *Cell Mol Life Sci* **77**, 1087-1101 (2020).

1575

1576 31. French, A. *et al.* *Drosophila* Bitter Taste(s). *Front Integr Neurosci* **9**, 58 (2015).

1577

1578 32. Montell, C. A taste of the *Drosophila* gustatory receptors. *Curr Opin Neurobiol* **19**,

1579 345-353 (2009).

1580

1581 33. Weiss, L.A., Dahanukar, A., Kwon, J.Y., Banerjee, D. & Carlson, J.R. The molecular and

1582 cellular basis of bitter taste in *Drosophila*. *Neuron* **69**, 258-272 (2011).

1583

1584 34. Kwon, J.Y., Dahanukar, A., Weiss, L.A. & Carlson, J.R. A map of taste neuron

1585 projections in the *Drosophila* CNS. *J Biosci* **39**, 565-574 (2014).

1586

- 1587 35. Marella, S. *et al.* Imaging taste responses in the fly brain reveals a functional map of  
1588 taste category and behavior. *Neuron* **49**, 285-295 (2006).  
1589
- 1590 36. Thorne, N., Chromey, C., Bray, S. & Amrein, H. Taste perception and coding in  
1591 *Drosophila*. *Curr Biol* **14**, 1065-1079 (2004).  
1592
- 1593 37. Wang, Z., Singhvi, A., Kong, P. & Scott, K. Taste representations in the *Drosophila*  
1594 brain. *Cell* **117**, 981-991 (2004).  
1595
- 1596 38. Dunipace, L., Meister, S., McNealy, C. & Amrein, H. Spatially restricted expression of  
1597 candidate taste receptors in the *Drosophila* gustatory system. *Curr Biol* **11**, 822-835  
1598 (2001).  
1599
- 1600 39. Itskov, P.M. *et al.* Automated monitoring and quantitative analysis of feeding  
1601 behaviour in *Drosophila*. *Nat Commun* **5**, 4560 (2014).  
1602
- 1603 40. Liu, W. *et al.* Enterococci Mediate the Oviposition Preference of *Drosophila*  
1604 *melanogaster* through Sucrose Catabolism. *Sci Rep* **7**, 13420 (2017).  
1605
- 1606 41. Zhai, Z., Boquete, J.P. & Lemaitre, B. Cell-Specific Imd-NF-kappaB Responses Enable  
1607 Simultaneous Antibacterial Immunity and Intestinal Epithelial Cell Shedding upon  
1608 Bacterial Infection. *Immunity* **48**, 897-910 e897 (2018).  
1609
- 1610 42. Guo, L., Karpac, J., Tran, S.L. & Jasper, H. PGRP-SC2 promotes gut immune  
1611 homeostasis to limit commensal dysbiosis and extend lifespan. *Cell* **156**, 109-122  
1612 (2014).  
1613
- 1614 43. Hedengren, M. *et al.* Relish, a central factor in the control of humoral but not cellular  
1615 immunity in *Drosophila*. *Mol Cell* **4**, 827-837 (1999).  
1616
- 1617 44. Harris, N. *et al.* The Innate Immune Receptor PGRP-LC Controls Presynaptic  
1618 Homeostatic Plasticity. *Neuron* **88**, 1157-1164 (2015).  
1619
- 1620 45. Harris, N., Fetter, R.D., Brasier, D.J., Tong, A. & Davis, G.W. Molecular Interface of  
1621 Neuronal Innate Immunity, Synaptic Vesicle Stabilization, and Presynaptic  
1622 Homeostatic Plasticity. *Neuron* **100**, 1163-1179 e1164 (2018).  
1623
- 1624 46. Stoven, S., Ando, I., Kadalayil, L., Engstrom, Y. & Hultmark, D. Activation of the  
1625 *Drosophila* NF-kappaB factor Relish by rapid endoproteolytic cleavage. *EMBO Rep* **1**,  
1626 347-352 (2000).  
1627
- 1628 47. Stanley, M., Ghosh, B., Weiss, Z.F., Christiaanse, J. & Gordon, M.D. Mechanisms of  
1629 lactic acid gustatory attraction in *Drosophila*. *Curr Biol* **31**, 3525-3537 e3526 (2021).  
1630
- 1631 48. Travassos, L.H. *et al.* Toll-like receptor 2-dependent bacterial sensing does not occur  
1632 via peptidoglycan recognition. *EMBO Rep* **5**, 1000-1006 (2004).  
1633

- 1634 49. Vaz, F. *et al.* Accessibility to Peptidoglycan Is Important for the Recognition of Gram-  
1635 Positive Bacteria in *Drosophila*. *Cell Rep* **27**, 2480-2492 e2486 (2019).  
1636
- 1637 50. Lopez-Requena, A. *et al.* Roles of Neuronal TRP Channels in Neuroimmune  
1638 Interactions. In: nd & Emir, T.L.R. (eds). *Neurobiology of TRP Channels*: Boca Raton  
1639 (FL), 2017, pp 277-294.  
1640
- 1641 51. Kim, H. *et al.* *Drosophila* Gr64e mediates fatty acid sensing via the phospholipase C  
1642 pathway. *PLoS Genet* **14**, e1007229 (2018).  
1643
- 1644 52. Mishra, D. *et al.* The molecular basis of sugar sensing in *Drosophila* larvae. *Curr Biol*  
1645 **23**, 1466-1471 (2013).  
1646
- 1647 53. Thistle, R., Cameron, P., Ghorayshi, A., Dennison, L. & Scott, K. Contact  
1648 chemoreceptors mediate male-male repulsion and male-female attraction during  
1649 *Drosophila* courtship. *Cell* **149**, 1140-1151 (2012).  
1650
- 1651 54. Fan, P. *et al.* Genetic and neural mechanisms that inhibit *Drosophila* from mating  
1652 with other species. *Cell* **154**, 89-102 (2013).  
1653
- 1654 55. Hardie, R.C. *et al.* Calcium influx via TRP channels is required to maintain PIP2 levels  
1655 in *Drosophila* photoreceptors. *Neuron* **30**, 149-159 (2001).  
1656
- 1657 56. Khush, R.S., Cornwell, W.D., Uram, J.N. & Lemaitre, B. A ubiquitin-proteasome  
1658 pathway represses the *Drosophila* immune deficiency signaling cascade. *Curr Biol* **12**,  
1659 1728-1737 (2002).  
1660
- 1661 57. Maillet, F., Bischoff, V., Vignal, C., Hoffmann, J. & Royet, J. The *Drosophila*  
1662 peptidoglycan recognition protein PGRP-LF blocks PGRP-LC and IMD/JNK pathway  
1663 activation. *Cell Host Microbe* **3**, 293-303 (2008).  
1664
- 1665 58. Gottar, M. *et al.* The *Drosophila* immune response against Gram-negative bacteria is  
1666 mediated by a peptidoglycan recognition protein. *Nature* **416**, 640-644 (2002).  
1667
- 1668 59. Takehana, A. *et al.* Peptidoglycan recognition protein (PGRP)-LE and PGRP-LC act  
1669 synergistically in *Drosophila* immunity. *EMBO J* **23**, 4690-4700 (2004).  
1670
- 1671 60. Paredes, J.C., Welchman, D.P., Poidevin, M. & Lemaitre, B. Negative regulation by  
1672 amidase PGRPs shapes the *Drosophila* antibacterial response and protects the fly  
1673 from innocuous infection. *Immunity* **35**, 770-779 (2011).  
1674
- 1675 61. Leulier, F., Rodriguez, A., Khush, R.S., Abrams, J.M. & Lemaitre, B. The *Drosophila*  
1676 caspase Dredd is required to resist gram-negative bacterial infection. *EMBO Rep* **1**,  
1677 353-358 (2000).  
1678
- 1679 62. Silbering, A.F., Bell, R., Galizia, C.G. & Benton, R. Calcium imaging of odor-evoked  
1680 responses in the *Drosophila* antennal lobe. *J Vis Exp* (2012).

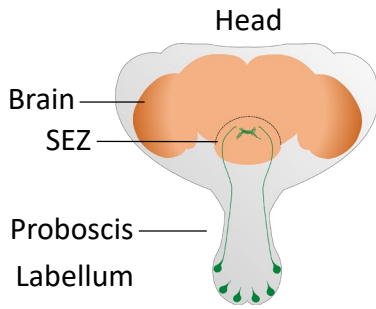
1681  
1682  
1683  
1684  
1685  
1686

63. Lopes, G. *et al.* Bonsai: an event-based framework for processing and controlling data streams. *Front Neuroinform* **9**, 7 (2015).

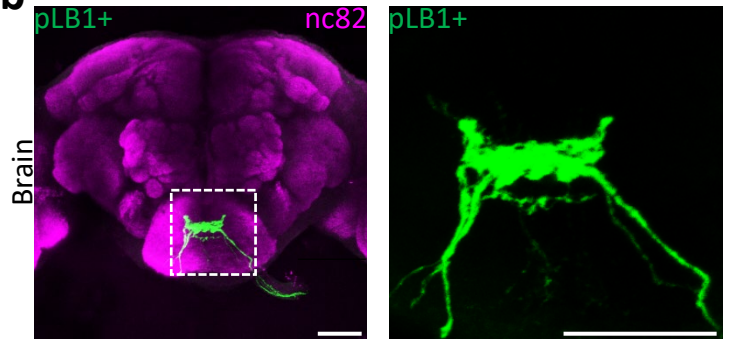


# Figure 1

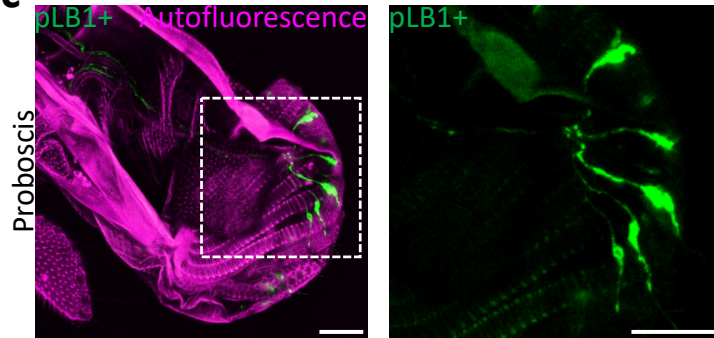
**a**



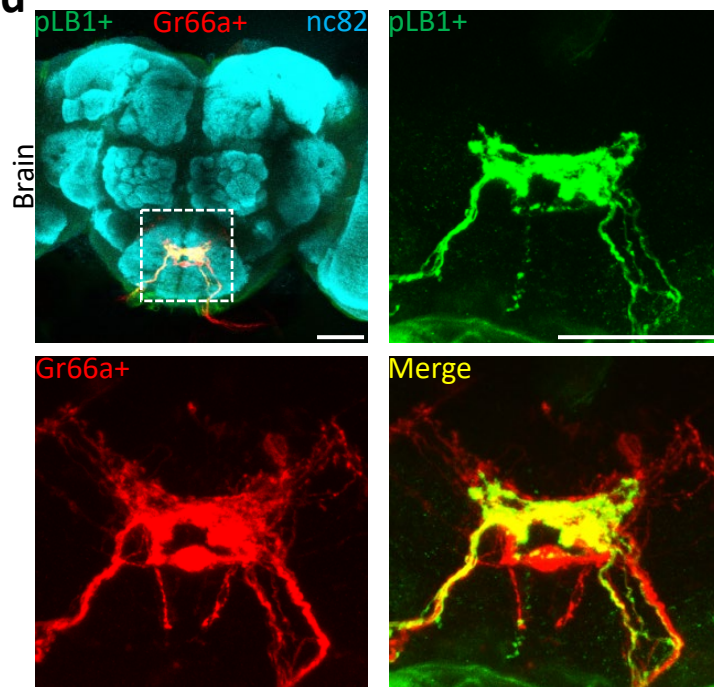
**b**



**c**



**d**



**e**

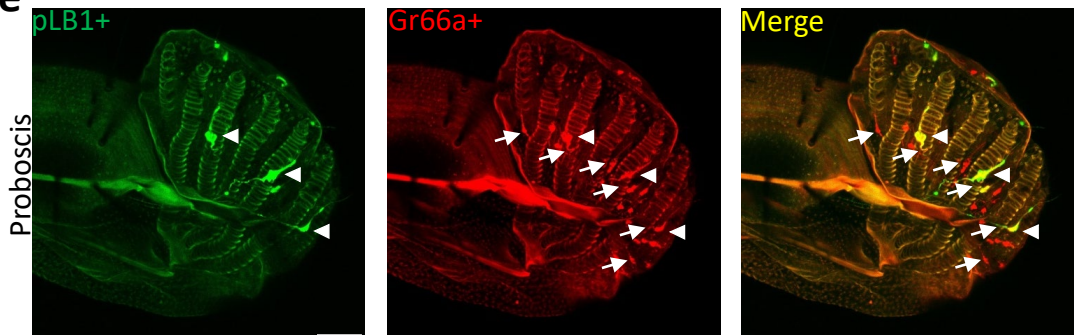


# Figure 2

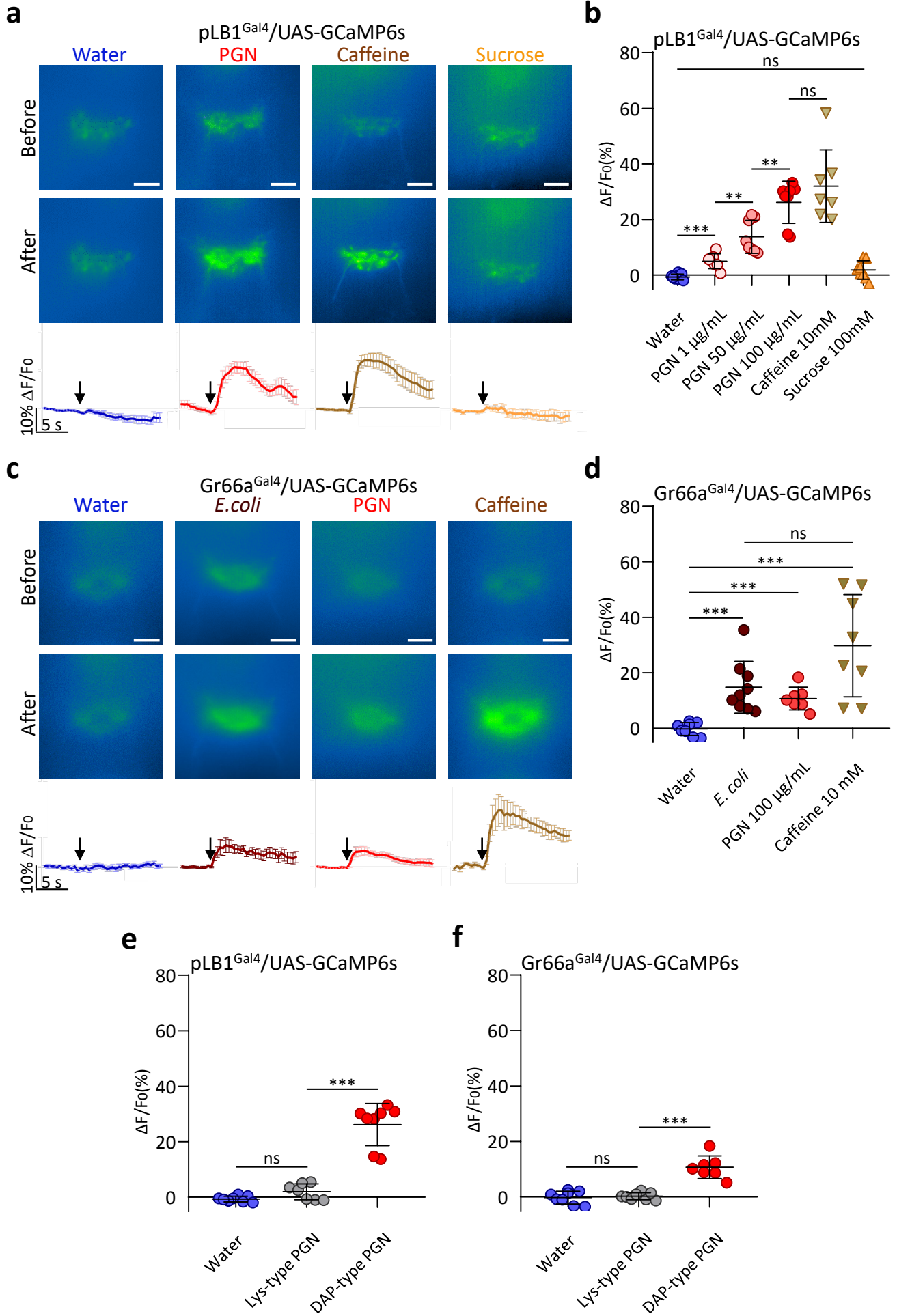
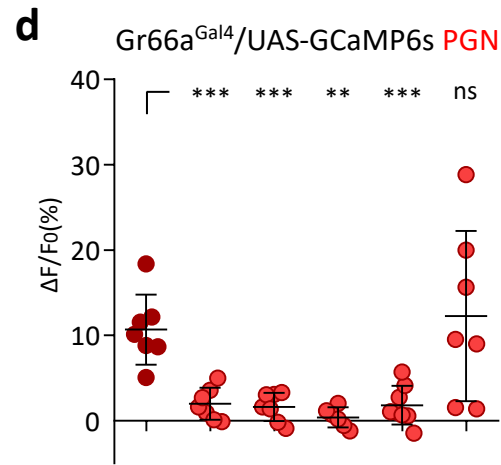
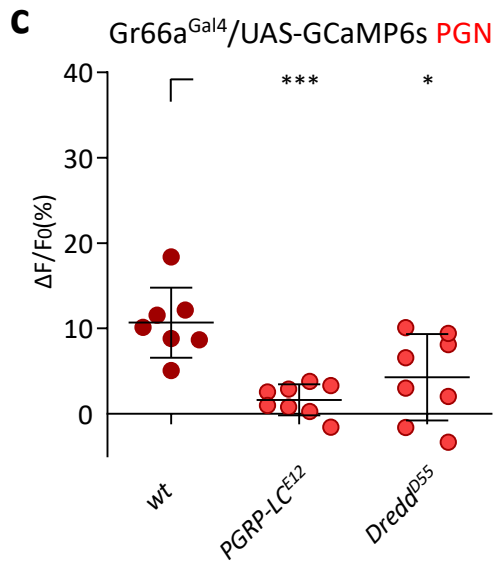
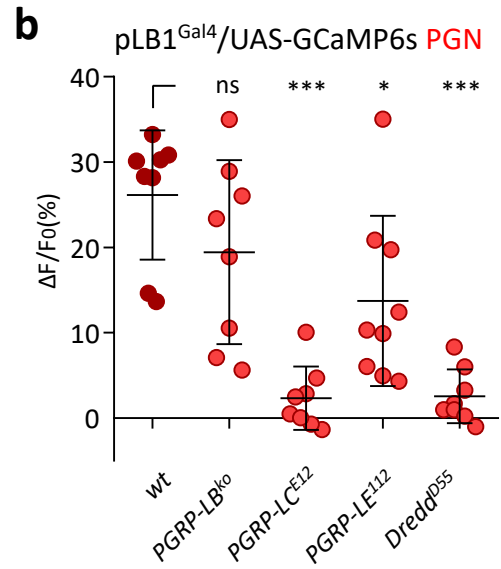
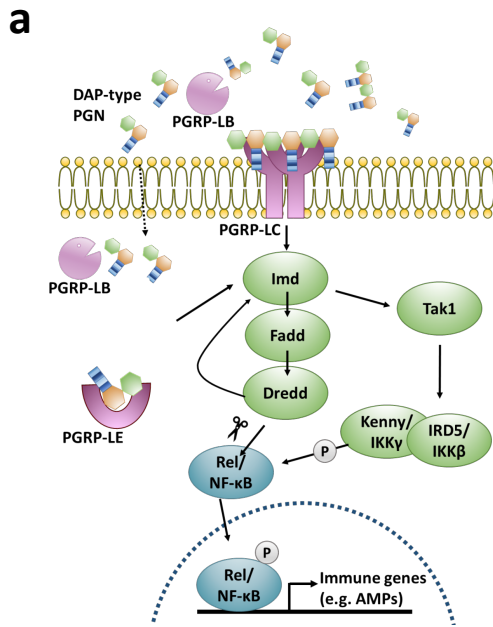




# Figure 3



UAS-PGRP-LC RNAi	-	+	-	-	-	-
UAS-Imd RNAi	-	-	+	-	-	-
UAS-Fadd RNAi	-	-	-	+	-	-
UAS-Dredd RNAi	-	-	-	-	+	-
UAS-Relish RNAi	-	-	-	-	-	+

# Figure 4

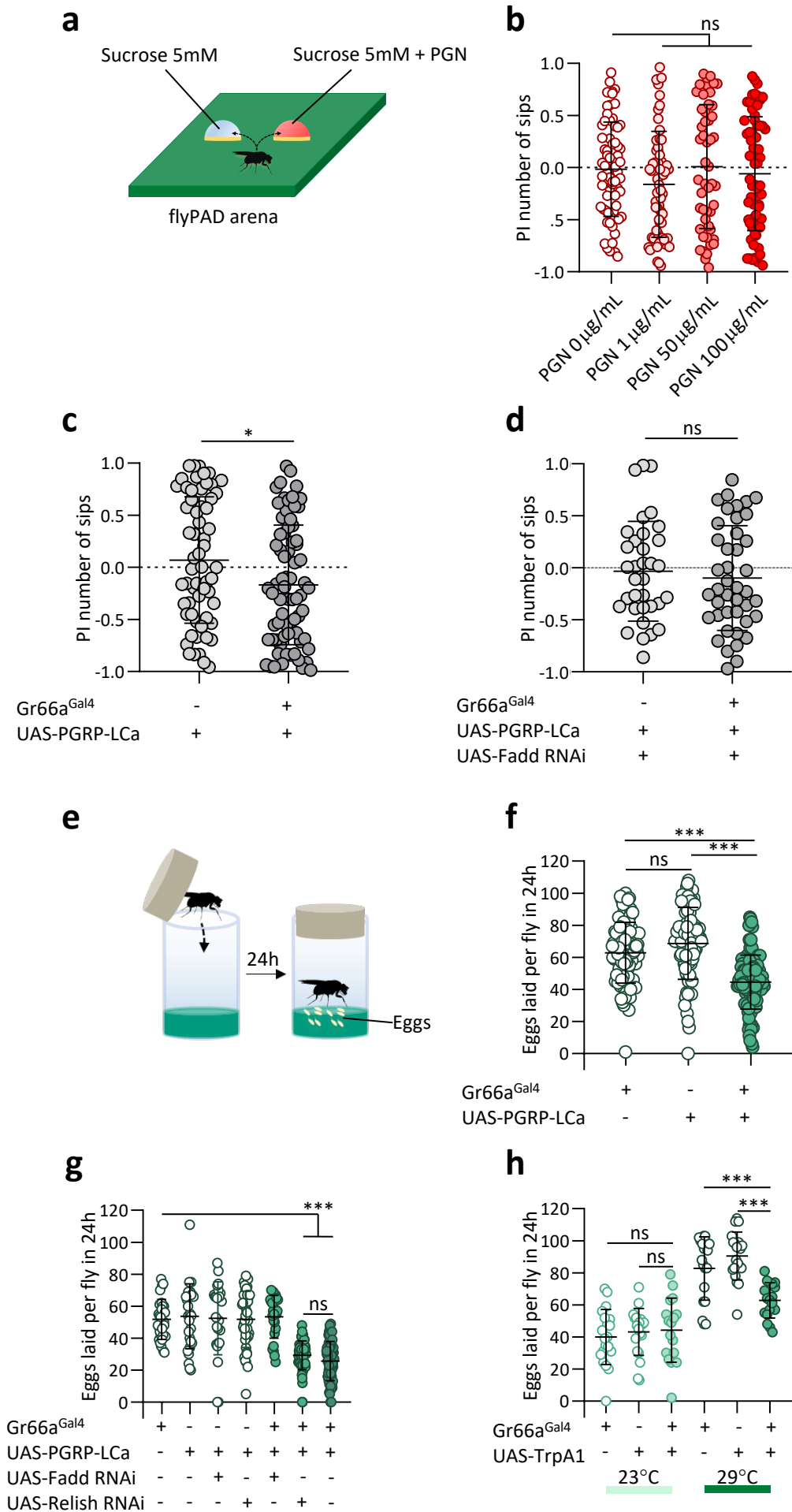


# Table 1

Number of observed pLB1+ neurons (event)	N events/ Total number of proboscis
3	5/32
4	6/32
5	11/32
6	6/32
7	3/32
8	1/32

# Table 2

Number of observed pLB1+ neurons	Number of observed Gr66a+ neurons	Number of observed pLB1+/Gr66a+ neurons
4	19	4
3	20	3
3	19	3
3	17	3
3	20	3
4	15	4